



Task <b>WFC3 Optical Stimulus</b>			
TITLE <b>CASTLE Exposure Time Calculator (Preliminary Version 0.9)</b>			
ORIGINATOR <b>Randal Telfer</b>	DATE <b>5/2/03</b>	REVIEWER <b>Brad Greeley</b>	DATE <b>5/6/03</b>

## 1 PROBLEM STATEMENT

An exposure time calculator is needed for test planning for the WFC3. This document describes the software developed for this purpose. Specifically, this document describes version 0.9 of the CASTLE exposure time calculator.

## 2 DESCRIPTION

### 2.1 Calculating the photon rate

The CASTLE exposure time calculator (ETC) models the throughput of most aspects of CASTLE and WFC3. Written out in the order that they will be discussed (which is mostly, but not quite, the order in the light path), the rate of photons detected by WFC3 is calculated as follows:

detected photons = lamp source  $\times$  grating efficiencies  $\times$  order sorting filters  $\times$  band pass  $\times$  neutral density filters  $\times$  off-axis parabolic mirror reflectivities  $\times$  coupling to fiber  $\times$  short fiber transmittance  $\times$  feed through fiber transmittance  $\times$  long fiber transmittance  $\times$  [integrating sphere efficiency  $\times$  extended target mirror  $\times$ ] telescope mirror reflectivities  $\times$  steering mirror reflectivities  $\times$  normalization  $\times$  WFC3 optics throughput  $\times$  WFC3 filter throughput  $\times$  WFC3 QE.

The terms in brackets are applicable only when the CASTLE integrating sphere is used. Each term in the above equation will now be discussed either individually or as a combination of terms.

#### 2.1.1 LAMP SOURCE $\times$ GRATING EFFICIENCIES

The first term in the model is the outputs of the lamps through the CASTLE double monochromator setup. The basic CASTLE monochromator setup can be seen in several other memos; for example, see WFC3-417-BWG-025 CASTLE Silicon Photodiode Flux Calibration. The outputs when the setup is used in double (high resolution) modes are measured by placing a detector next to the exit slit. The monochromators are set in each of the available double monochromator modes, and spectra are acquired over the anticipated useful range of each mode with a 1 nm FWHM band pass. At wavelengths shorter than 900 nm a Newport 818-UV silicon photodiode (NUV), serial number 2599, is used, while at longer wavelengths we use a Newport 818-IR germanium photodiode (NIR), serial number 6604. The spectra of the Xenon and QTH lamps, converted to photons  $\text{s}^{-1}$ , are shown in Figure 1 and Figure 2. In this configuration, the NUV detector should intercept much, but probably not all, of the emerging flux. Thus the photon rate plotted here indicates a substantial but unknown fraction of the total flux. The data from

the NIR detector have been renormalized to the level of the NUV detector to account for the difference in detector area. The spectra were acquired with appropriate order-sorting filters, and the spectra shown have been corrected for the transmission of these filters, but not for the grating efficiencies, as discussed in the next paragraph. Implicit in this discussion is the presence of nine surfaces of  $\text{Al}(\text{MgF}_2)$  in the two monochromators, including the gratings.

To calculate the output in single monochromator mode or mirror mode, we need to divide by the efficiencies of the gratings used in acquiring the spectra in Figure 1 and Figure 2. These grating efficiencies were obtained from paper plots supplied by Oriel and are plotted in Figure 3. Since the low resolution UV grating is not used by itself the efficiency of that grating is not shown. The spectra obtained by dividing the double mode spectra by the appropriate high resolution grating efficiency are shown in Figure 4 for the Xenon lamp. There is a small discrepancy between the Single UVIS fluxes derived from double UVIS and double VIS modes, with a maximum of around 40%. The two agree well at around 500 nm, so we use the spectrum derived from the double UVIS data short of 500 nm and double VIS data at longer wavelengths, resulting in a smooth single UVIS spectrum. The same is done for the QTH lamp.

Similarly we can use the single UVIS and single IR data to find the mirror mode spectra by dividing by the low resolution grating efficiencies. We plot the results in Figure 5, here using the QTH lamp as an example. There is a larger discrepancy in this case, up to a factor of 4. For the mirror model we use the single UVIS data up to 1060 nm, where the two agree, and single IR data for 1060 nm and above. The derived spectra for the single modes and mirror are only estimates and need not be exact, since the results for these modes will be renormalized in the 'normalization' part of the calculation to match the observed fluxes. Note that the efficiency plots supplied by Oriel are only typical, and not actual measurements of the gratings used, so we would expect some disagreement.

#### 2.1.2 ORDER SORTING FILTERS

The transmission of the order sorting filters were measured by taking spectra at the output of the monochromator slit with and without the filters in the wavelength region where the transmission changes strongly until it levels out, then is assumed to be constant to longer wavelengths. The transmissions so derived are shown in Figure 6.

#### 2.1.3 BAND PASS

In double monochromator mode, the band pass is determined by the convolution of the entrance and exit slits of the second monochromator. Since these exit and entrance slits are always set to the same widths, the result is a triangular band pass. When the slits are all the way open with a width of 2000 microns, the resulting band pass is 13 nm FWHM. The FWHM scales linearly with the slit width, as does the peak of the band pass.

In single mode the widths of the entrance and exit slits to the second monochromator do not have an effect on the band pass, since the band pass is essentially determined by the width of the entrance slit to the first monochromator, which is never changed. The band pass is thus fixed as a rectangle with a width of about 125 nm. The normalization of the

band pass again scales linearly with the slit widths. This normalization is true of the mirror mode as well.

#### 2.1.4 NEUTRAL DENSITY FILTERS

Two neutral density filter wheels are placed in the light path between the two off-axis parabolic mirrors that image the monochromator exit slit on the fiber. The use of these filters is discussed in WFC3-577-BWG-004 Procedure for ND Filter Use. The optical densities as measured by the manufacturer are plotted in Figure 7 for filter wheel 1. The filters in filter wheel 2 are essentially identical.

#### 2.1.5 OFF-AXIS PARABOLIC MIRROR REFLECTIVITIES $\times$ COUPLING TO FIBER $\times$ SHORT FIBER TRANSMITTANCE

These three contributions are closely related and most easily measured as a combination. To measure the combined contribution of these terms to the system throughput, we measure the output at the monochromator exit slit and then the output of the short fiber with the fiber stage in the correct position for that particular fiber. Figure 8 shows the results for the point target fibers. IRPT2 and UVPT2 are assumed to be identical to IRPT1 and UVPT1 since they are the exactly the same model fiber. Figure 9 shows the same plots for the integrating sphere fibers. Only one of the eight channels of each integrating sphere bundle was used for this measurement, and thus the total combined throughput of the entire bundle will be many times larger. This is just a numerical factor, assumed to be constant with wavelength, which will be accounted for in the 'normalization' step.

#### 2.1.6 FEED THROUGH FIBER TRANSMITTANCE

The feed through fiber transmittance is measured as described in WFC3-417-RCT-003 Throughput of CASTLE Fibers for Ultraviolet Extended Targets. Only one fiber of each type was measured. The measured transmittances are plotted in Figure 10.

#### 2.1.7 LONG FIBER TRANSMITTANCE

The transmittance of 10m fibers is described in WFC3-167-BWG-007 Ceramoptec Fiber Transmission. The transmittance of the 21' fibers being used on CASTLE are calculated by scaling from the 10m fiber measurements and shown in Figure 11.

#### 2.1.8 INTEGRATING SPHERE EFFICIENCY

The integrating sphere efficiency is a function of the geometry of the sphere and the reflectance of the Spectralon coating. The efficiency, according to Labsphere, is given by:

$$e = \frac{r A_{\text{exit}} / A_{\text{sphere}}}{1 - (r(1 - A_{\text{all}} / A_{\text{sphere}}))},$$

where  $r$  is the reflectivity of the Spectralon,  $A_{\text{exit}}$  is the area of the exit port,  $A_{\text{sphere}}$  is the area of the inside of the sphere, and  $A_{\text{all}}$  is the area of all the ports. For the CASTLE sphere,  $A_{\text{sphere}} = 2.919 \times 10^5 \text{ mm}^2$ ,  $A_{\text{exit}} = 3.364 \times 10^3 \text{ mm}^2$ , and  $A_{\text{all}} = 3.369 \times 10^3 \text{ mm}^2$ .

For reflectivities estimated from paper plots from Labsphere, the efficiency curve for the CASTLE 12" integrating sphere is plotted in

Figure 12.

#### 2.1.9 EXTENDED TARGET MIRROR

The extended target mirror is coated with  $\text{Al}(\text{MgF}_2)$  and has a typical reflectivity curve.

#### 2.1.10 TELESCOPE MIRROR REFLECTIVITIES

The refurbishment of the CASTLE telescope, including the cleaning of the mirrors and recoating of the primary, is described in WFC3-577-RKP-001 Telescope Disassembly, Pinning, Strip/Coat, Reassembly, and Retest Report. The measured reflectivity curves are plotted in Figure 13. Because we only have a measured reflectivity for the secondary at wavelengths shorter than 600 nm, at longer wavelengths we use a typical  $\text{Al}(\text{MgF}_2)$  reflectivity.

#### 2.1.11 STEERING MIRROR REFLECTIVITIES

The reflectivity curves for the steering mirrors M3 and M4 have been measured from witness samples and are typical for  $\text{Al}(\text{MgF}_2)$ .

#### 2.1.12 NORMALIZATION

At this point in the light path we have reached the CASTLE monitor detectors and can therefore compare to measured data. The normalization actually consists of three parts: (1) a general factor for each fiber to account for certain geometric factors that have been ignored, particularly the fraction of light exiting the fibers that contributes to the image (or in the case of the integrating sphere,  $1 \text{ cm}^2$  of the image); (2) for single modes and mirror mode, an adjustment to the overall shape to account for inconsistencies with the observed data; and (3) for the integrating sphere, a factor of the pixel area to convert the flux to photons per pixel.

The normalization factor for each fiber is calculated by comparing simulated fluxes in double modes to measured ones. For the UV fibers we use an average of double UVIS fluxes between 210 and 600 nm, while for the VISIR fibers we use double VIS fluxes between 350 and 800 nm.

Despite all the detail put into the ETC, there are still differences between the measured fluxes and predicted ones in the single modes, with a peak of around a factor of 4 in both directions. To correct for this we take the ratio of the measured values to predicted ones as a function of wavelength and multiply the single mode fluxes by an interpolation of the resulting values in order to match the measurements. The mirror mode fluxes are corrected using the same data.

We multiply by the pixel area to convert to flux per pixel. This cannot be taken into account by the previous normalization because it is a function of the channel being used. For the UVIS channel, we use a pixel area of  $1.224 \times 10^{-6} \text{ cm}^2$ , while for the IR detector

we use an area of  $1.275 \times 10^{-5} \text{ cm}^2$ , where these values are as seen by CASTLE including the demagnification of the WFC3 optics.

#### 2.1.13 WFC3 OPTICS THROUGHPUT $\times$ WFC3 FILTER THROUGHPUT

The WFC3 optics throughput is the same as used by the WFC3 ETC at the STScI web site; see <http://www.stsci.edu/instruments/wfc3/>. The throughputs are plotted in Figure 14. The throughputs for the various WFC3 filters are also retrieved from this web site.

#### 2.1.14 WFC3 QE

The WFC3 ETC site lists several detector QE curves for each channel. The UVIS QE curve we use is an average of CCD18, CCD178, CCD40, and CCD50, while the IR QE curve is an average of FPA32, FPA34, FPA45, FPA50, and FPA58. The QEs that we use are plotted in Figure 15.

### 2.2 Signal-to-Noise and Exposure Time Calculations

The S/N is calculated according to standard CCD noise calculations using the calculated photon rate, as well as the exposure time and CCD parameters supplied by the user. The signal is given by:

$$\text{signal (ADU)} = \frac{n_{\text{phot}} t}{g},$$

where  $n_{\text{phot}}$  is the number of detected photons per second,  $t$  is the total integration time in seconds, and  $g$  is the gain in  $e^-$  per ADU. The noise is given by

$$\text{noise (ADU)} = \sqrt{\frac{n_{\text{phot}} t}{g^2} + \frac{n_{\text{pix}} D t}{g^2} + \frac{n_{\text{exp}} n_{\text{pix}} r^2}{n_{\text{bin}}}},$$

where  $n_{\text{pix}}$  is the number of pixels in the region over which the calculation is being performed,  $D$  is the dark current in  $e^-$  per second,  $n_{\text{exp}}$  is the number of sub-exposures,  $r$  is the read noise in  $e^-$ , and  $n_{\text{bin}}$  is the number of pixels per bin if on-chip binning is being used.

If the integrating sphere is being used,  $n_{\text{pix}}$  is the number of pixels per bin, or one pixel if no binning is used.

If a point target is being used, the number of pixels is determined by the size of the image.

For UVPT1 and IRPT1 the image is assumed to be a 200-micron diameter circle. The number of pixels is then given by

$$n_{\text{pix}} = \pi d^2 / 4 A_{\text{pix}},$$

where  $d$  is 200 microns and  $A_{\text{pix}}$  is the pixel area.

For UVPT2 and IRPT2 the user-specified PSF diameter is used

$$n_{\text{pix}} = p d_{\text{psf}}^2 / 4,$$

where  $d_{\text{psf}}$  is the diameter of the PSF in pixels.

An exposure time is calculated from the S/N by solving the quadratic equation in  $t$  defined by the S/N. The calculator also finds the number of electrons per pixel in the image and ADU per pixel (or bin if on-chip binning is used). The number of electrons and ADU include both the signal and the dark current.

### 2.3 CASTLE Monitor Detector Fluxes

The detector fluxes are calculated by multiplying the flux per nm by the detector sensitivity at each wavelength, then summing up to find the total output. The actual measured preamp gains and chopped signal to DC signal conversion factors are used, and the PMT count rate is corrected for non-linearity at high count rates to give the observed count rate.

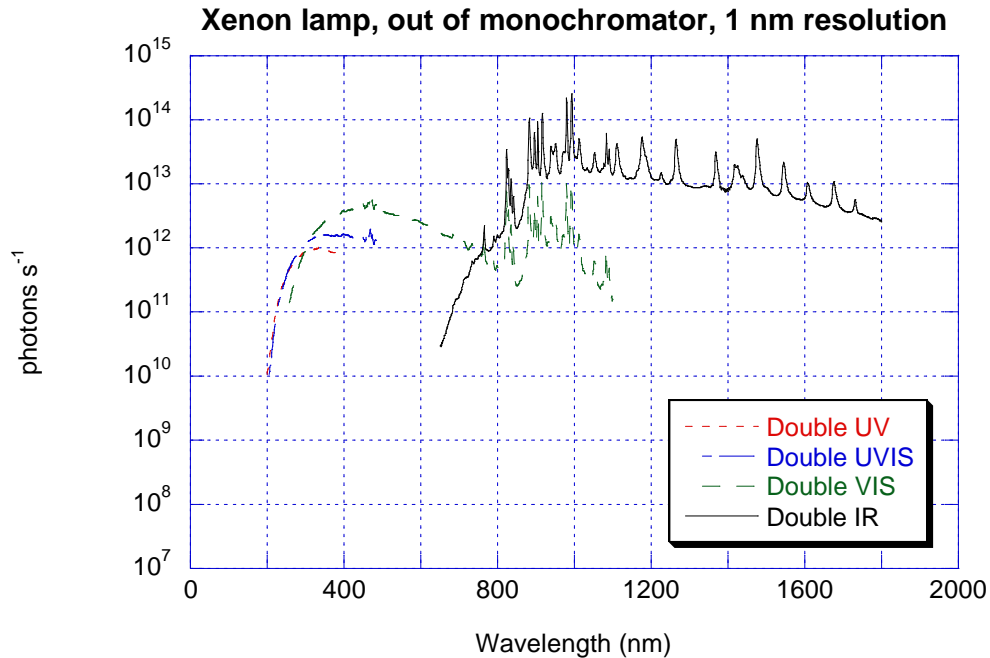


Figure 1 – Spectra of the Xenon lamp at the monochromator exit slit in various double monochromator modes. Spectra in the IR are renormalized to the data from the silicon detector to account for the smaller size.

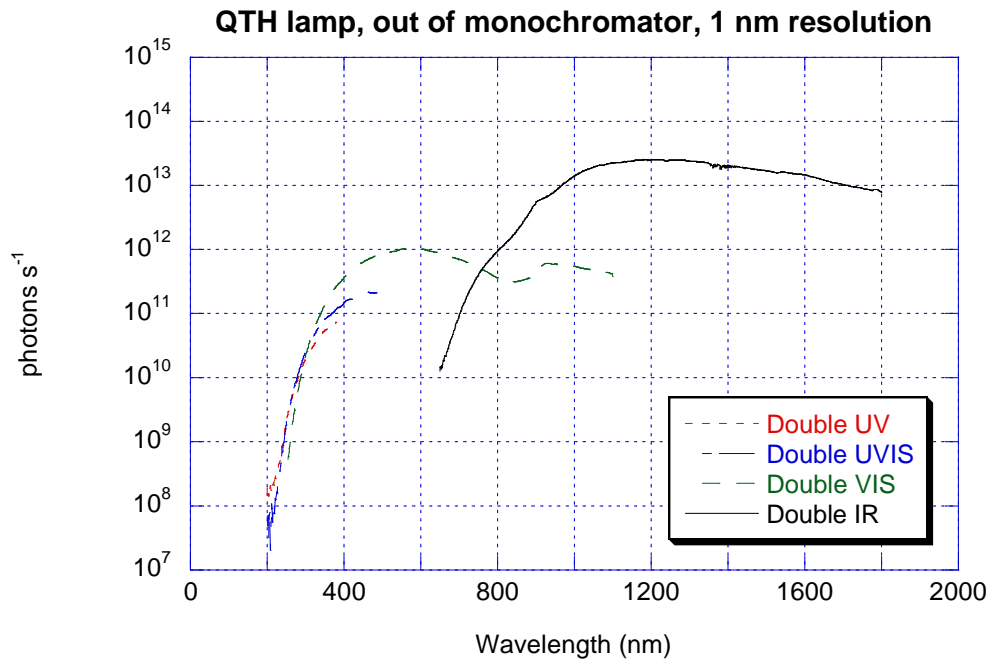


Figure 2 - Spectra of the QTH lamp at the monochromator exit slit.

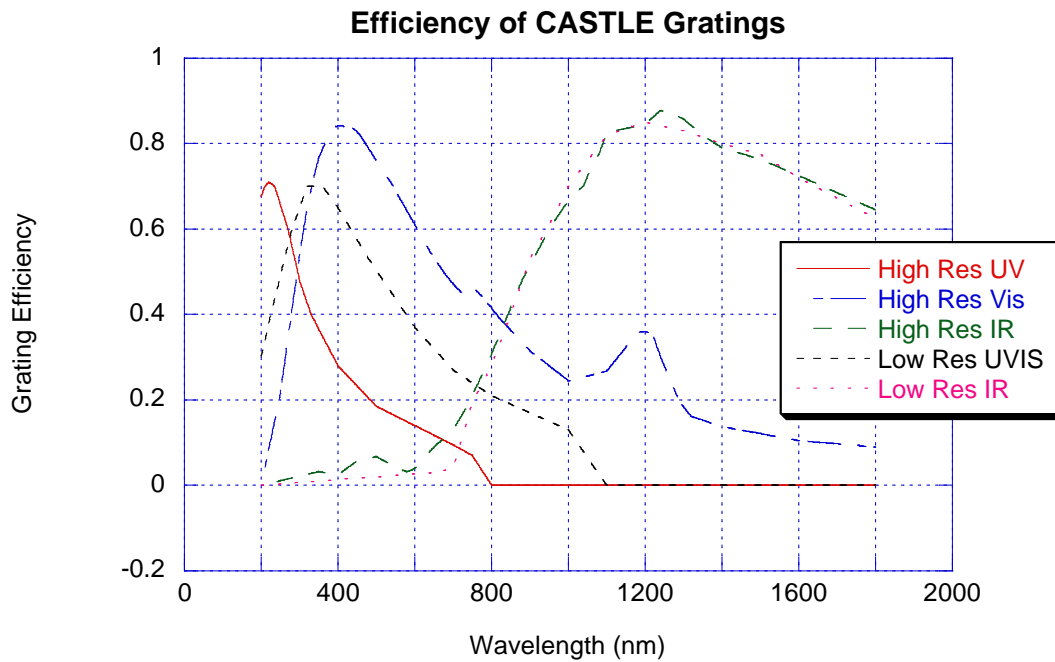


Figure 3 - Efficiency of CASTLE gratings as determined from paper plots from Oriel.

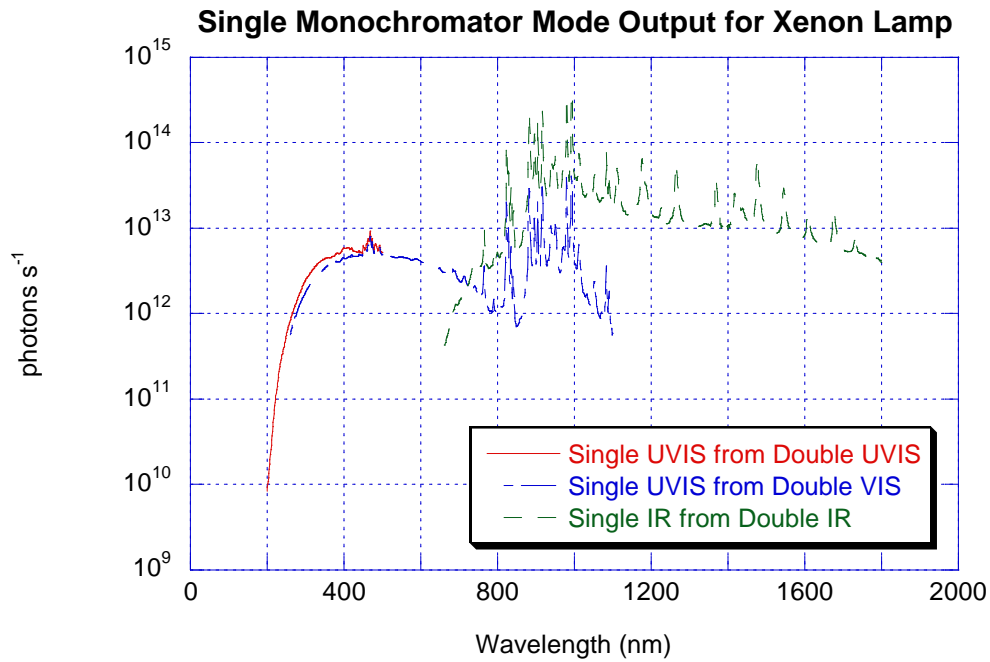


Figure 4 - Single mode outputs for the Xenon lamp as derived by dividing the spectra in Figure 1 by the appropriate grating efficiencies from Figure 3. For the model single UVIS we use the data derived from double UVIS at wavelengths shorter than 500 nm and double VIS at wavelengths longer than 500 nm.

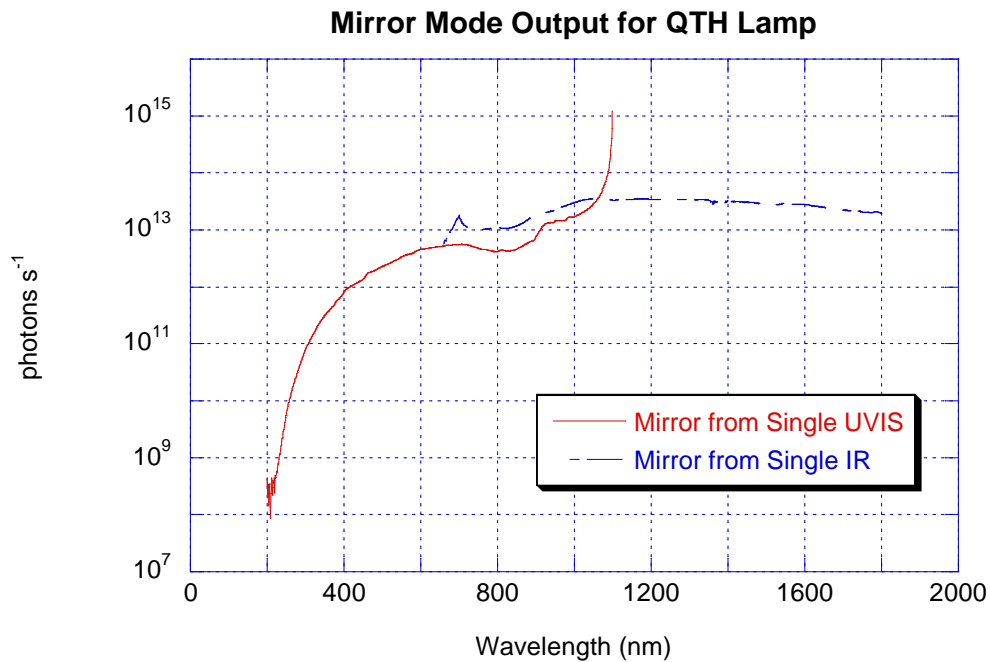


Figure 5 - Mirror mode output from the QTH lamp as determined from the single UVIS data and the single IR data. For the model we use the single UVIS data up to 1060 nm, where the two match, and use single IR at longer wavelengths.



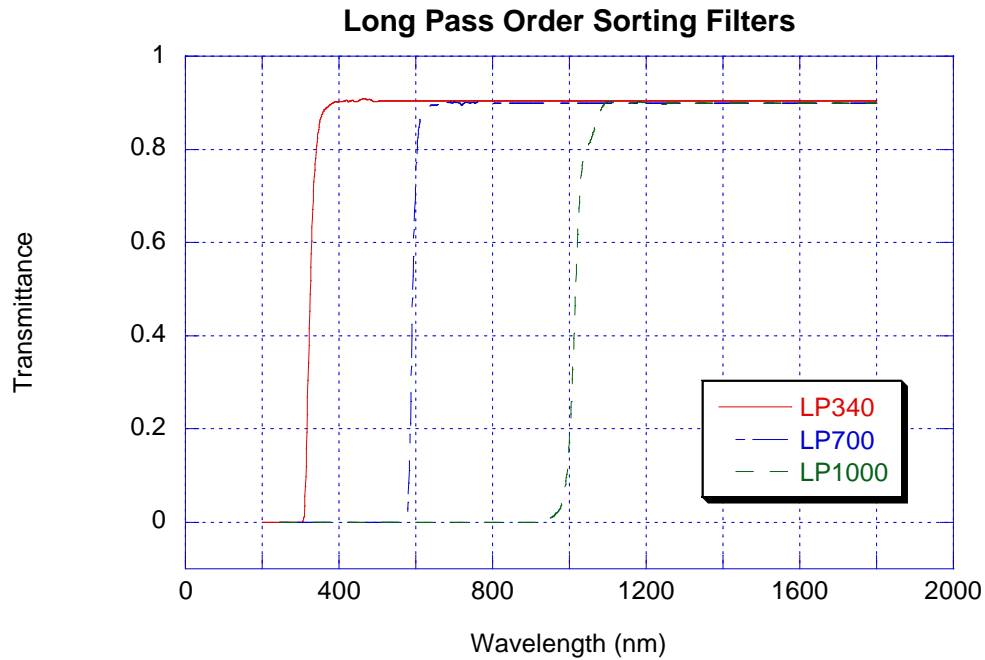


Figure 6 – Transmittance of the order sorting filters placed in between the two CASTLE monochromators.

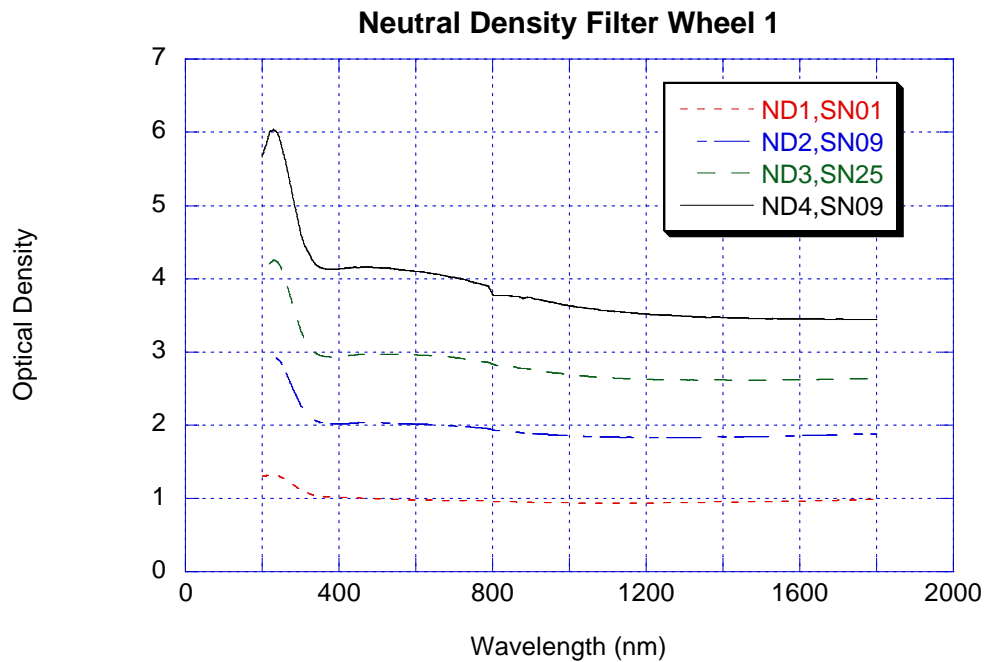


Figure 7 - Optical densities of neutral density filters in filter wheel 1. The filters in filter wheel 2 are virtually identical.

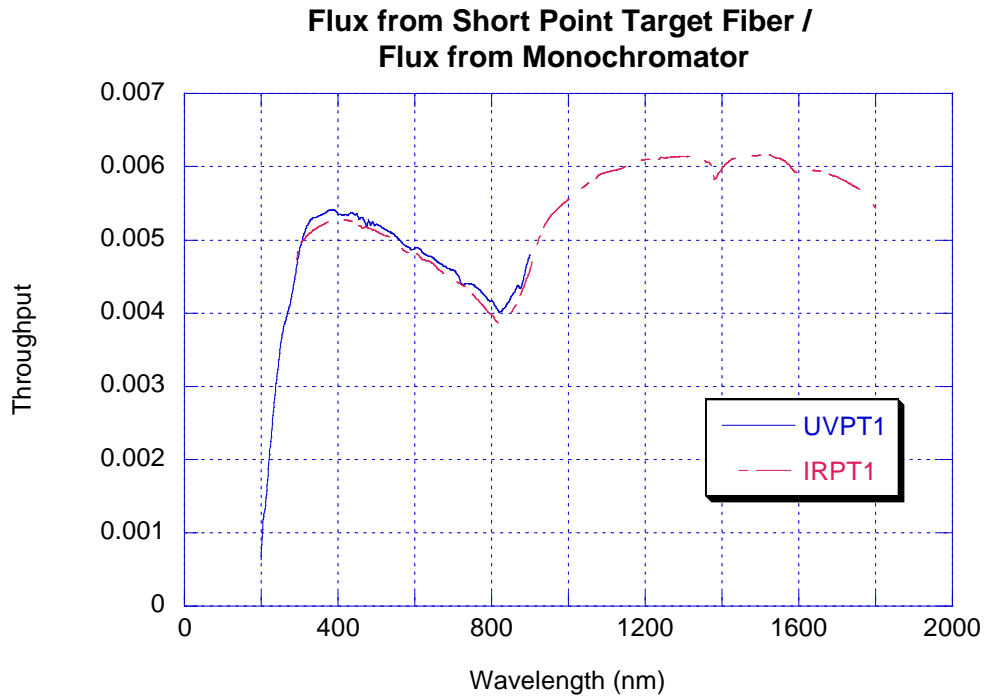


Figure 8 - Combined throughput of the off-axis parabolic mirrors, coupling to the fibers, and the short fiber transmittance for the point target fibers.

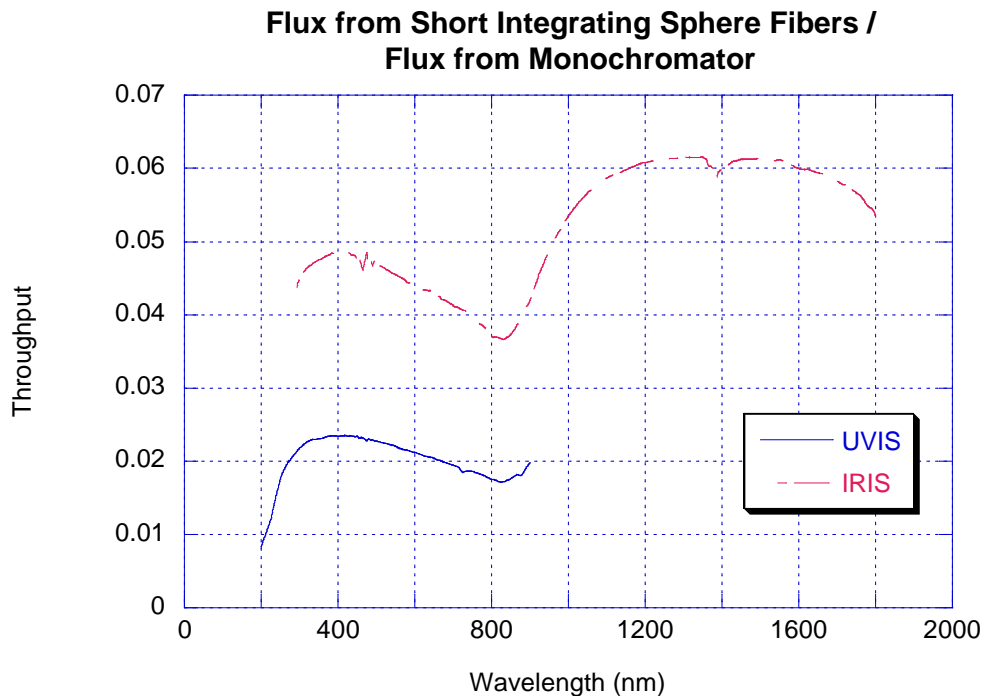


Figure 9 - Same as Figure 8 for the integrating sphere fibers. Only one channel was used for each, and thus the difference in normalization is due to the variation in flux from channel to channel. The throughputs are much larger than the point targets because larger fibers are used.

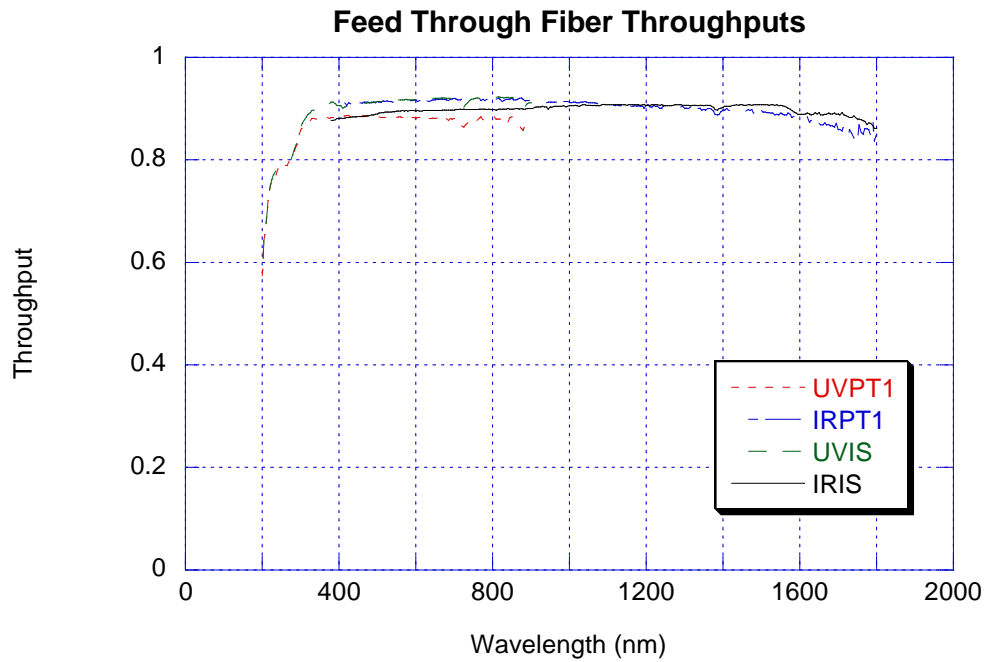


Figure 10 - Throughput of CASTLE feed through fibers.

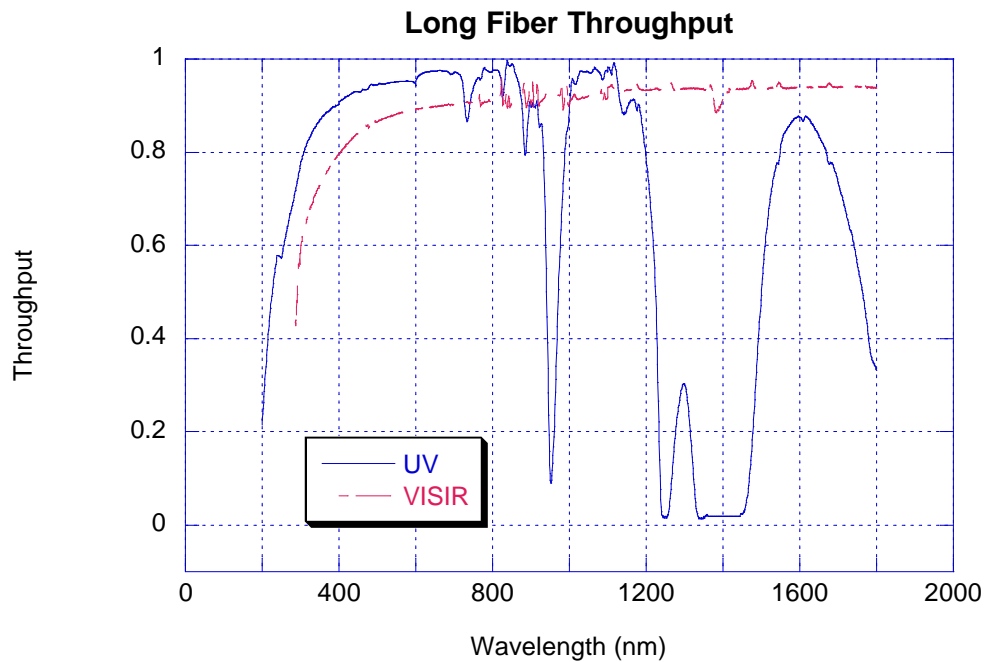


Figure 11 - Throughput of 21' CASTLE fibers.

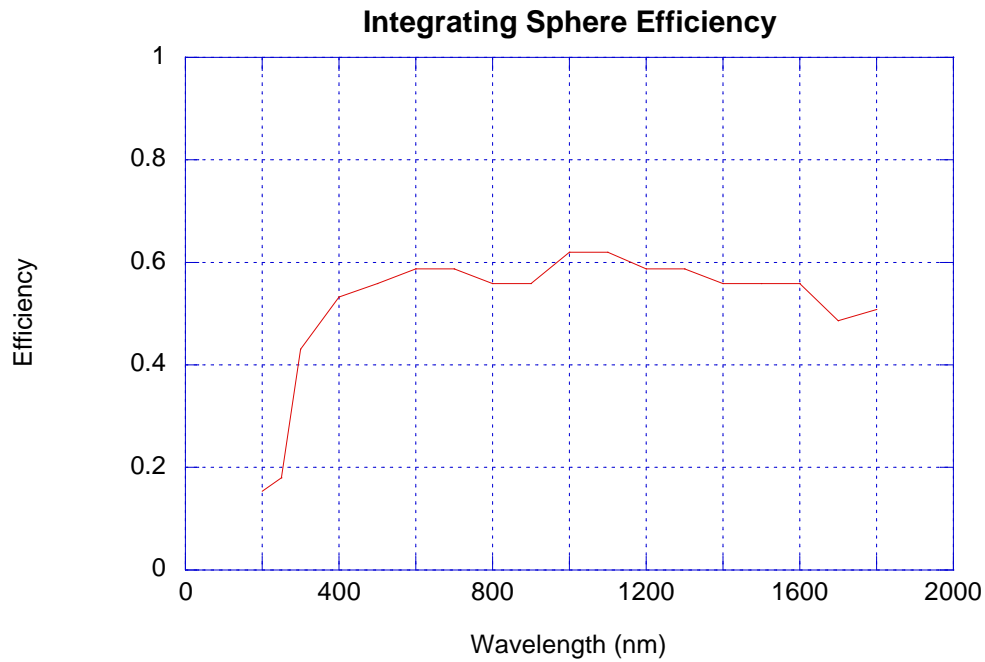


Figure 12 - Ratio of output to input power for the CASTLE 12" integrating sphere as a function of wavelength.

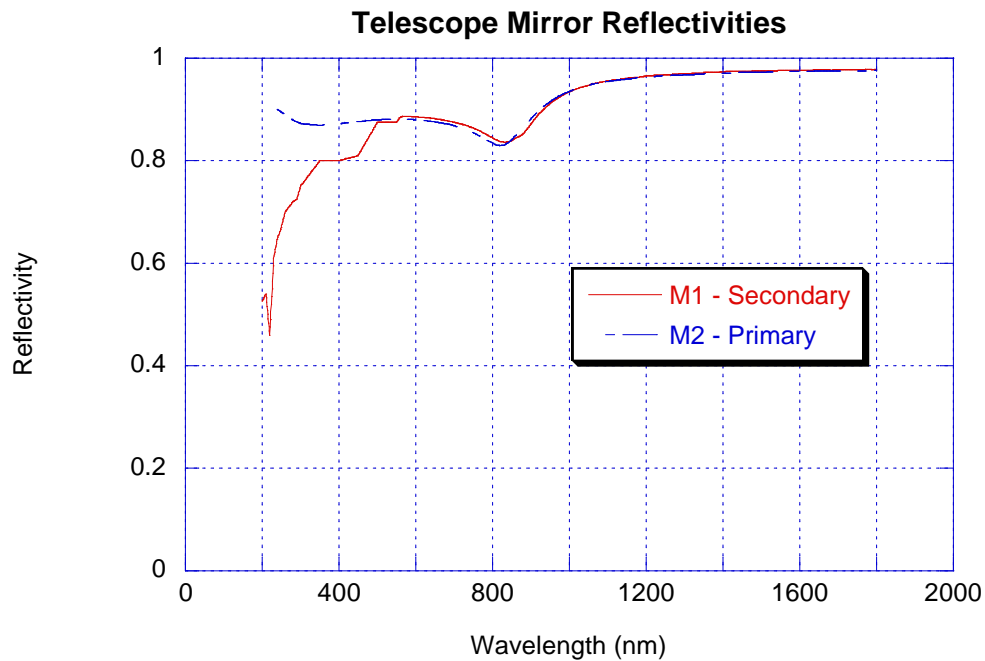


Figure 13 - Reflectivities of stimulus telescope mirrors after refurbishment. The secondary reflectivity was measured only up to 600 nm so we assign a typical Al(MgF<sub>2</sub>) reflectivity at longer wavelengths.

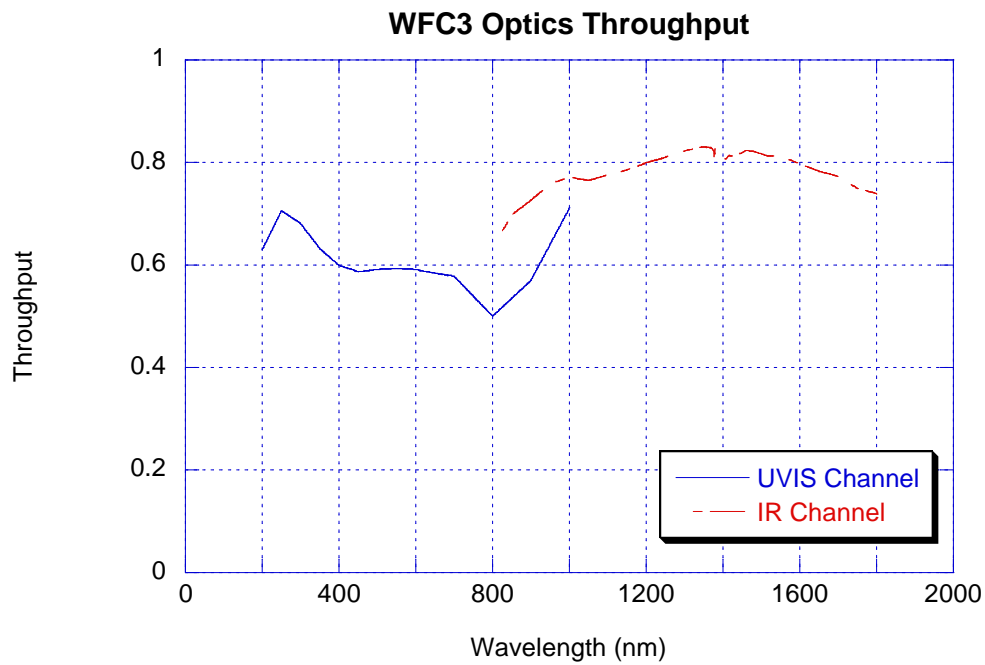


Figure 14 - WFC3 optics throughput as used by the WFC3 ETC.

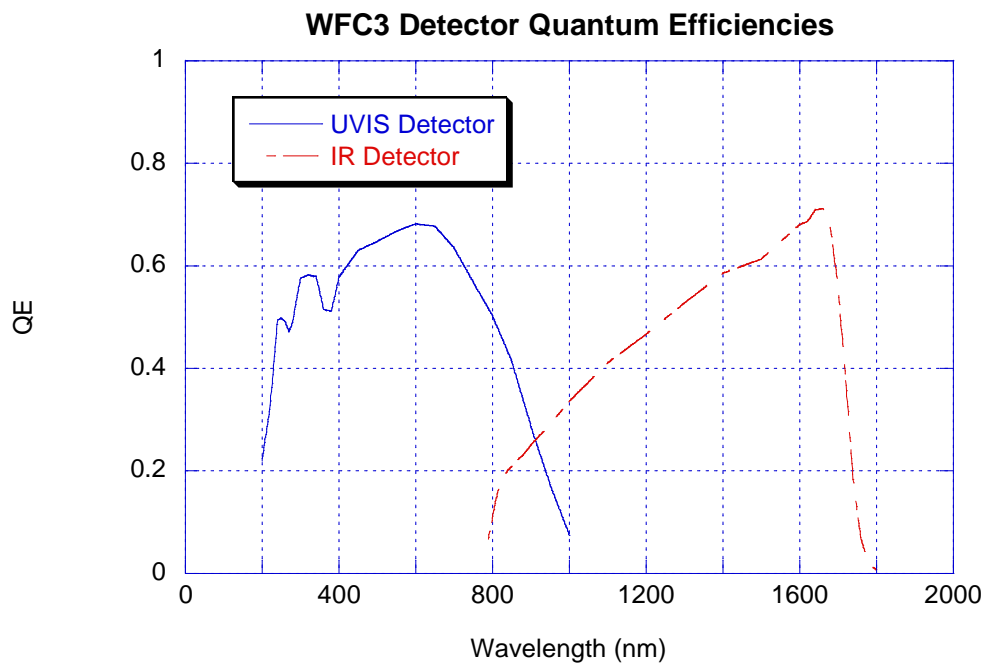


Figure 15 - WFC3 detector quantum efficiencies used by the ETC. These are an average of several QE curves listed as being used by the WFC3 ETC.

### 3 USING THE CALCULATOR

Figure 16 shows the user panel for the CASTLE ETC, written in Microsoft Excel, with the separate sections labeled. Here we outline a likely manner in which the user may use the calculator.

1. Set up the WFC3 in the configuration to be tested, including choosing the correct channel and filter.
2. Set the CASTLE parameters into a proper configuration to perform the test.
3. Set the exposure time calculator up in the desired manner. For example, set up to calculate the time necessary to accumulate 70000 electrons per pixel.
4. Observe the results. Forms of output include the rate of incident on and being detected by WFC3, both in spectral and integrated form; signals on the CASTLE monitor detectors; and the results of the calculator (the required exposure time or the resulting S/N, depending on which aspect of the calculator is of interest.)
5. Adjust the CASTLE parameters, if necessary and possible, to achieve the desired result. For example, a common situation will be that the exposure times are very short (due to a very bright source.) The user may choose different neutral density filters to achieve the desired brightness.

The remainder of this section will discuss in more detail each of the boxes on the CASTLE ETC user panel.

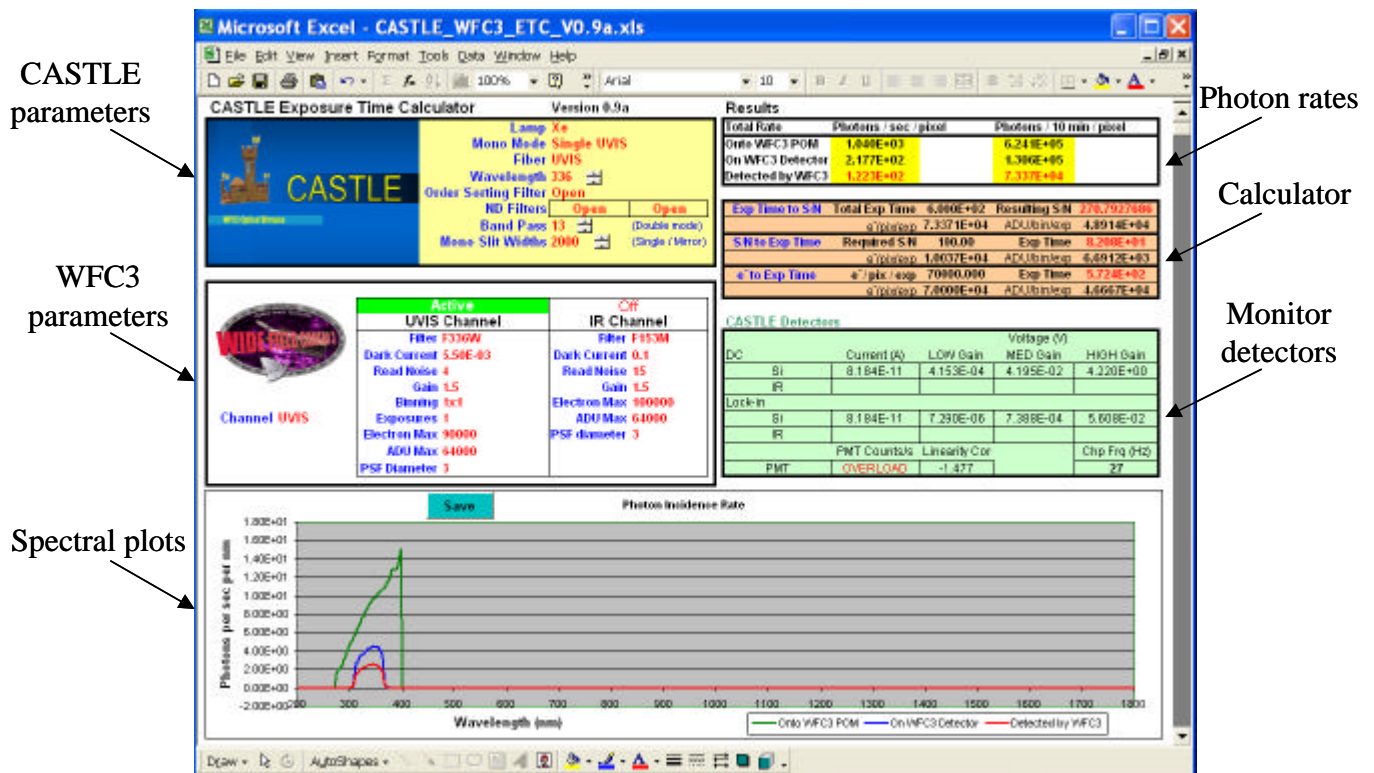


Figure 16 - CASTLE ETC user panel.

### 3.1 WFC3 Parameters

The WFC3 parameter box allows the user to set the parameters specific to WFC3. This box is shown in Figure 17. Many of the parameters are characteristics of the detector that will probably be set rarely or only once. These include the dark current for each detector, specified in electrons / pixel / sec, the read noise per pixel of the detector in electrons, the gain of the readout amplifiers in electrons / ADU, the maximum number of electrons per pixel, and the maximum number of ADU per bin. The user also has the option of using on-chip binning or breaking up the total exposure time into multiple exposures for the UVIS channel.

The maximum number of electrons is intended to be not necessarily the full-well value but whatever value the user does not wish to exceed (probably where the response becomes non-linear). The maximum number of ADU is whatever maximum value can be read out and recorded by the system. The only consequence of these numbers is that in the 'Calculator' box, where the electrons per pixel and ADU per bin are calculated, the background of the corresponding fields will turn red to warn the user that these values have been exceeded.

The channel is selected below the WFC3 logo. A green bar indicating 'Active' appears above whatever channel is being used to remind the user of which parameters are relevant. As with other parameters that are chosen from a list, such as the WFC3 filters, the user is presented with a drop-down menu when the parameter is clicked. To change parameters that can take on any value, such as the read noise, the user simply clicks on the parameter and types in a value as normal.

The PSF diameter is only relevant when using the pinhole apertures of IRPT2 or UVPT2. For these apertures the diameter of the WFC3 PSF determines the spot size, and this is used to for the S/N calculation.


 <p>Channel UVIS</p>	<div>Active</div> <div>UVIS Channel</div> <div>Filter F336W</div> <div>Dark Current 5.50E-03</div> <div>Read Noise 4</div> <div>Gain 1.5</div> <div>Binning 1x1</div> <div>Exposures 1</div> <div>Electron Max 90000</div> <div>ADU Max 64000</div> <div>PSF Diameter 3</div>	<div>Off</div> <div>IR Channel</div> <div>Filter F153M</div> <div>Dark Current 0.1</div> <div>Read Noise 15</div> <div>Gain 1.5</div> <div>Electron Max 100000</div> <div>ADU Max 64000</div> <div>PSF diameter 3</div>
---	---	---

Figure 17 - WFC3 parameter control box in the CASTLE exposure time calculator.

### 3.2 CASTLE Parameters

The CASTLE parameter box, shown in Figure 18, is where most of the action of the CASTLE ETC takes place, since there are many parameters that can be changed. Every possible configuration may not be defined for all wavelengths, so the user should be careful to set up the CASTLE in a reasonable configuration. Otherwise, the results may not be valid.



Figure 18 - CASTLE parameter control box in the CASTLE ETC.

We now briefly discuss each parameter and recommendations for the usage of each.

#### 3.2.1 LAMP

There are two lamps to choose from on CASTLE, a xenon lamp and a quartz tungsten halogen lamp. The outputs of the two lamps can be compared by viewing Figure 1 and Figure 2. At wavelengths shorter than 400 nm, the xenon lamp is much brighter and is the obvious choice. At wavelengths longer than 800 nm, the xenon lamp contains many emission lines, and the QTH, which is much smoother and nearly as bright or brighter, is probably the best choice for the source. In between either lamp may be used depending on the requirements. The xenon lamp is brighter in this region but also contains a few emission lines, particular around 470 nm.

#### 3.2.2 MONO MODE

There are seven supported monochromator modes for CASTLE: double UV, double UVIS, double VIS, double IR, single UVIS, single IR, and mirror. The single modes have a rectangular band pass with a width of 125 nm and the double modes have an adjustable triangular band pass with a maximum width of 13 nm FWHM. The output of the various modes is shown in Figure 1, Figure 2, Figure 4, and Figure 5. The output is only defined for each mode in the wavelength range shown in the plots. It is generally preferable to use the most efficient mode at any given wavelength. The choice of double mode vs. single mode vs. mirror will probably be determined by the width of the WFC3 filter.

#### 3.2.3 FIBER

There are three types of targets the user may choose: a bare 200-micron fiber point target, a pinhole point target, and the integrating sphere. In addition, there are UV and VISIR versions of each of these, accounting for the six possible positions on the fiber stage. The fibers called 'UVPT1' and 'IRPT1' are the bare 200-micron fibers, while 'UVPT2' and 'IRPT2' are the pinholes, where UVPT2 is a 5-micron pinhole and IRPT2





is 10 microns. The relative throughput of the VISIR vs. UV fibers is determined mostly by the long fibers, shown in Figure 11. Though the UV fiber is better at shorter wavelengths, it has absorption features at longer wavelengths. The feedthrough fibers and short fibers are not defined for the UV fibers at wavelengths longer than 900 microns, so the UV fiber should not be used at longer wavelengths in the ETC. The VISIR fibers are defined from 280-1800 nm.

#### 3.2.4 WAVELENGTH

This parameter is simply the central wavelength of the band pass. It has no effect in mirror mode.

#### 3.2.5 ORDER SORTING FILTERS

The appropriate order-sorting filters will be selected automatically by the stimulus team during testing, but these filters are not chosen automatically by the ETC so the user must select them explicitly. By default, in double modes we plan to use the LP340 filter for wavelengths from 380 to 650 nm, the LP700 filter from 650 to 1100 nm, and the LP1000 filter for wavelengths longer than 1100 nm.

#### 3.2.6 ND FILTERS

There are two neutral density filter wheels in the light path between the monochromator exit slit and the fibers that can be used to adjust the signal level in roughly order-of-magnitude increments. A maximum attenuation of two ND4 filters (around eight orders of magnitude) may be used.

#### 3.2.7 BAND PASS

The band pass may be adjusted in double modes only and has a maximum value of 13 nm FWHM. Changing this parameter has no effect in single modes or mirror mode.

#### 3.2.8 SLIT WIDTHS

In single modes and mirror mode changing the entrance and exit slit widths of the second monochromator changes the light level. (In double modes this changes the band pass and falls under the previous heading.) This parameter is included as part of the simulation but should be used sparingly. To reduce the flux by a large amount, use the ND filters instead.

### 3.3 Spectral Plots and Results Box

The output is shown in the spectral plots and in the results box. The spectral plots show the number of photons per second per nm incident on the WFC3 pickoff mirror, striking the WFC3 detector, and detected by WFC3. The results box shows these values summed over all wavelengths and also converted to photons per 10 min since these units are used in the requirements document.

There is a 'Save' button above the spectral plots. This will save the three curves shown on the plot in numerical form to an Excel file, along with a header describing the state of the system. The user is presented with a dialog box for choosing the filename.

### 3.4 Calculator

There are three ways to use the CASTLE ETC, and all three are always in use simultaneously. The first task is to calculate the S/N that results from a given total exposure time. The S/N is calculated per pixel (or bin) if the integrating sphere is used, and for the entire spot if a point target is used. The second task is the inverse, calculating the exposure time that is necessary to achieve a given S/N. Finally, the calculator finds the exposure time necessary to collect a given number of electrons per sub-exposure in each pixel in the region of interest. For each calculation, the calculator also shows the number of electrons per pixel per sub-exposure and the number of ADU per bin per sub-exposure in the region of interest. The 'region of interest' includes all pixels when using the integrating sphere, but only the pixels exposed to light when using a point target. These numbers include both signal and dark current. If the number of electrons / pixel / exposure or ADU / bin / exposure exceed the maximum values given in the WFC3 parameter box, the background of the corresponding number field will turn red as a warning.

<b>Exp Time to S/N</b>	<b>Total Exp Time</b>	<b>6.000E+02</b>	<b>Resulting S/N</b>	<b>270.7927686</b>
	e <sup>-</sup> /pix/exp	7.3371E+04	ADU/bin/exp	4.8914E+04
<b>S/N to Exp Time</b>	<b>Required S/N</b>	<b>100.00</b>	<b>Exp Time</b>	<b>8.208E+01</b>
	e <sup>-</sup> /pix/exp	1.0037E+04	ADU/bin/exp	6.6912E+03
<b>e<sup>-</sup> to Exp Time</b>	<b>e<sup>-</sup> / pix / exp</b>	<b>70000.000</b>	<b>Exp Time</b>	<b>5.724E+02</b>
	e <sup>-</sup> /pix/exp	7.0000E+04	ADU/bin/exp	4.6667E+04

Figure 19 - The calculator box on the CASTLE ETC user panel.

### 3.5 Monitor Detectors

The last box on the CASTLE ETC user panel, shown in Figure 20, indicates the signals that would be seen on the CASTLE monitor detectors. The measured voltages for the silicon and IR detectors include the actual measured gains of the CASTLE preamps and, for the lock-in measurements, the correct conversion from DC to chopped signal. In the example, there is no signal listed for the IR detector since there is no signal, as the photons are in the UV. The count rate for the PMT includes a correction for non-linearity due to the finite resolution of the counter. If the observed count rate for the PMT exceeds  $10^7$  counts s<sup>-1</sup>, which is our imposed safe limit, then the count rate reads as 'OVERLOAD'. The only parameter on this box is the chopping frequency, which can be changed from 27 to 17 Hz in the ETC. It is not changeable during stimulus operations, however, where it will be fixed at 17 Hz. The chopping frequency will change the observed signal on the lock-in slightly.



TECHNICAL SERVICES DIVISION  
Technical Memorandum

5/2/03  
WFC3-577-RCT-005

CASTLE Detectors

DC		Voltage (V)		
		Current (A)	LOW Gain	HIGH Gain
Si		8.184E-11	4.153E-04	4.195E-02
IR				
Lock-in				
Si		8.184E-11	7.290E-06	7.388E-04
IR				
		PMT Counts/s	Linearity Cor	Chp Frq (Hz)
PMT		OVERLOAD	-1.477	27

Figure 20 - CASTLE monitor detector box displaying the signal on each detector.